*Anal. Chem.* **2002,** *74,* 1572−1577

# Laser Ablation Construction of On-Column Reagent Addition Devices for Capillary Electrophoresis

Yohannes H. Rezenom, Joseph M. Lancaster, III, Jason L. Pittman, and S. Douglass Gilman*

*Department of Chemistry, University of Tennessee, Knoxville, Tennessee 37996-1600*

**A simple and reproducible technique for constructing perfectly aligned gaps in fused-silica capillaries has been developed for postcolumn reagent addition with capillary electrophoresis. This technique uses laser ablation with the second harmonic of a Nd:YAG laser (532 nm) at 13.5 mJ/pulse and a repetition rate of 15 Hz to create these gaps. A capillary is glued to a microscope slide and positioned at the focal point of a cylindrical lens using the focused beam from a laser pointer as a reference. Gaps of 14.0 ± 2.2 $\mu$m ($n$ = 33) at the bore of the capillary are produced with a success rate of 94% by ablation with 400 pulses. This simple method of gap construction requires no micromanipulation under a microscope, hydrofluoric acid etching, or use of column fittings. These structures have been used for reagent addition for postcolumn derivatization with laser-induced fluorescence detection and have been tested for the separation of proteins and amino acids. Detection limits of $6 \times 10^{-7}$ and $1 \times 10^{-8}$ M have been obtained for glycine and tranferrin, respectively. Separation efficiencies obtained using these gap reactors range from 38 000 to 213 000 theoretical plates.**

On-line addition of chemical reagents has played an essential role in the development of capillary electrophoresis (CE) as a versatile separation technique at the heart of a wide variety of new analytical methods. Initially, on-line reagent addition was used for postcolumn derivatization with fluorescence detection.[1−5] On-line addition of chemical reagents has been central to the development of chemiluminescence detection for CE.[6,7] Additional applications of on-line reagent addition for CE include electrochemical detection,[8,9] bioaffinity detection,[10,11] enzyme assays,[12] and electroosmotic flow monitoring.[13]

A variety of interfaces have been developed for on-line reagent addition with CE.[1,6,7] A recent review by Zhu and Kok divides on-line reagent addition device designs into four categories: coaxial reactors, gap reactors, free solution reactors, and sheath flow cuvette reactors.[1] The coaxial reactor is one of the earliest reported designs and one of the most commonly employed designs.[1,3,6,7] The separation capillary is inserted into a reaction capillary, and the reagent is introduced into the reaction capillary by pressure or an applied potential. Gap reactors have also been used extensively and will be discussed in more detail later.[1,6,7,14] Free solution reactors, where the reaction and detection take place in the buffer reservoir at the detection end of the capillary, have also been used occasionally.[1,6,7,15] Sheath flow cuvettes have been developed for CE primarily to reduce light scattering for fluorescence detection,[16] but this design has been used less frequently for postcolumn reagent addition.[1,6,7,17−19] Microlithographically constructed analytical devices in planar glass and polymer substrates have been used for on-column reagent addition integrated with electrophoretic separations.[20−25] Microfabricated devices in planar substrates offer superior design flexibility compared to capillaries. However, there is an important role for on-line reagent addition with capillary-based electrophoretic systems, especially for applications that require small-volume sampling and specialized applications where the economy of scale advantages of microfabricated systems do not apply.

The gap reactor is a simple and effective device for on-line reagent addition for CE separations.[1,6,7,14,26] Reagents are added on-line through a small gap (typically 3−100 $\mu$m) between two capillaries based on either diffusion or a higher flow rate in the

* Corresponding author: (e-mail) sdgilman@utk.edu; (tel) (865) 974-3465; (fax) (865) 974-3454.

(1) Zhu, R.; Kok, W. T. *J. Pharm. Biomed. Anal.* **1998**, *17*, 985−999.
(2) Waterval, J. C. M.; Lingeman, H.; Bult, A.; Underberg, W. J. M. *Electrophoresis* **2000**, *21*, 4029−4045.
(3) Rose, D. J.; Jorgenson, J. W. *J. Chromatogr.* **1988**, *447*, 117−131.
(4) Pentoney, S. L.; Huang, X.; Burgi, D. S.; Zare, R. N. *Anal. Chem.* **1988**, *60*, 2625−2629.
(5) Tsuda, T.; Kobayashi, Y. *J. Chromatogr.* **1988**, *456*, 375−381.
(6) Huang, X. J.; Fang, Z. *Anal. Chim. Acta* **2000**, *414*, 1−14.
(7) Kuyper, C.; Milofsky, R. *Trends Anal. Chem.* **2001**, *20*, 232−240.
(8) Cassidy, R. M.; Lu, W.; Tse, V. *Anal. Chem.* **1994**, *66*, 2578−2583.
(9) Zhou, J.; Lunte, S. M. *Anal. Chem.* **1995**, *67*, 13−18.
(10) Abler, J. K.; Reddy, K. R.; Lee, C. S. *J. Chromatogr., A* **1997**, *759*, 139−147.
(11) Feltus, A.; Hentz, N. G.; Daunert, S. *J. Chromatogr., A* **2001**, *918*, 381−392.
(12) Emmer, A.; Roeraade, J. *J. Chromatogr., A* **1994**, *662*, 375−381.
(13) Lee, T. T.; Dadoo, R.; Zare, R. N. *Anal. Chem.* **1994**, *66*, 2694−2700.
(14) Albin, M.; Weinberger, R.; Sapp, E.; Moring, S. *Anal. Chem.* **1991**, *63*, 417−422.
(15) Rose, D. J. *J. Chromatogr.* **1991**, *540*, 343−353.
(16) Cheng, Y. F.; Wu, S.; Chen, D. Y.; Dovichi, N. J. *Anal. Chem.* **1990**, *62*, 496−503.
(17) Zhao, J. Y.; Labbe, J.; Dovichi, N. J. *J. Microcolumn Sep.* **1993**, *5*, 331−339.
(18) Oldenburg, K. E.; Xi, X.; Sweedler, J. V. *Analyst* **1997**, *122*, 1581−1585.
(19) Nirode, W. F.; Staller, T. D.; Cole, R. O.; Sepaniak, M. J. *Anal. Chem.* **1998**, *70*, 182−186.
(20) Polson, N. A.; Hayes, M. A. *Anal. Chem.* **2001**, *73*, 312A−319A.
(21) Bruin, G. J. M. *Electrophoresis* **2000**, *21*, 3931−3951.
(22) Jacobson, S. C.; Koutny, L. B.; Hergenroder, R.; Moore, A. W.; Ramsey, J. M. *Anal. Chem.* **1994**, *66*, 3472−3476.
(23) Fluri, K.; Fitzpatrick, G.; Chiem, N.; Harrison, D. J. *Anal. Chem.* **1996**, *68*, 4285−4290.
(24) Jacobson, S. C.; McKnight, T. E.; Ramsey, J. M. *Anal. Chem.* **1999**, *71*, 4455−4459.
(25) Liu, Y.; Foote, R. S.; Jacobson, S. C.; Ramsey, R. S.; Ramsey, J. M. *Anal. Chem.* **2000**, *72*, 4608−4613.
(26) Kuhr, W. G.; Licklider, L.; Amankwa, L. *Anal. Chem.* **1993**, *65*, 277−282.



10.1021/ac015693w CCC: $22.00 
Published on Web 02/23/2002

reaction capillary relative to the separation capillary. Separated compounds migrate across the gap from the separation capillary into the reaction capillary. Flow in the reaction capillary can be generated by either an applied potential or a pressure difference between the gap buffer reservoir and the other end of the reaction capillary. The gap reactor design has been successfully applied to on-line reagent addition for postcolumn derivatization,[1,2,14] chemiluminescence detection,[6,7] electrochemical detection,[8,9] bioaffinity detection,[10] and enzyme assays.[27] These devices have also been used for transfer of digested peptides from an enzyme-modified capillary to a separation capillary,[28] as a detection cell for confocal laser-induced fluorescence (LIF),[29] and for continuous single-cell introduction and lysis.[30] A related approach has been used for postcolumn reagent addition for continuous electrophoretic separations in thin channels.[31]

The difficulty of reactor construction is a common limitation of the two most popular designs for on-line reagent addition for CE, of coaxial reactors and gap reactors, the two most popular designs for on-line reagent addition for CE. The best performance for coaxial reactors systems has been achieved using capillaries etched with hydrofluoric acid.[1,3,11,32] The etched capillaries are extremely fragile, and the etching procedure requires careful attention and uses dangerous reagents. The performance of gap reactors is critically dependent on the alignment of the two capillaries and the distance between them.[1,8,26,33,34] The first reported gap reactor was constructed by aligning two capillaries 10−50 $\mu$m apart in a machined reactor cell and securing the capillaries in place using ferrule-based fittings.[14] This alignment and spacing is difficult to accomplish in practice. Micromanipulators have been used to align capillaries under a microscope.[8,26,28] Gap reactors have been aligned by inserting the capillaries into permeable tubing and by using small wires to guide alignment of the capillaries.[1,9,30,35−37] Two related approaches have been developed to simplify gap construction.[33,38] Both approaches are based on cleaving a single, secured capillary to create a gap reactor. While these two approaches have been used to produce functional reactors, they both require manual cutting of the capillary under a microscope. It is difficult to control the size of the gap using both approaches. Development of a simple and reproducible method for constructing coaxial reactors or gap reactors will make it more practical to use on-line reagent addition for CE and will expand the development of new analytical methods based on on-line reagent addition.

One of the earliest reports of on-line reagent addition for CE used laser ablation for device construction.[4] Pentoney and co-workers used a $CO_2$ laser to drill a hole through the bore of a 75-$\mu$m-i.d./375-$\mu$m-o.d. capillary. This hole was then used to manually interface two additional capillaries to the drilled capillary to form a cross connector which was used for postcolumn derivatization and LIF detection. Despite this early report and advances made in laser-based micromachining of fused silica,[39−42] the application of laser ablation for construction of capillary electrophoretic devices has been limited. Girault and co-workers reported the application of UV laser ablation with an excimer laser to construct a microfluidic device in a polymer substrate.[43,44] Recently, Lunte and Osbourn used a $CO_2$ laser to etch a series of holes along the length of a capillary.[45] These holes were used to construct a cellulose acetate decoupler for electrochemical detection with CE.

In this paper, we present a reproducible method based on laser ablation for constructing small (<20 $\mu$m), perfectly aligned gaps between two capillaries without micromanipulation under a microscope, HF etching, or use of column fittings. The reproducibility of this gap construction technique has been investigated. The performance of these capillary gaps for on-line reagent addition for CE has been examined by using the capillary gaps to perform postcolumn derivatization for LIF detection of amino acids and proteins.

## EXPERIMENTAL SECTION

**Gap Construction.** A 50-$\mu$m-i.d./220-$\mu$m-o.d. fused-silica capillary (SGE; Austin, TX) was secured to a microscope slide (Fisher Scientific; Pittsburgh, PA) at two points for gap construction with 5 Minute Epoxy (ITWDevcon; Danvers, MA) using a mount designed to position the capillary at a reproducible distance (~950 $\mu$m) from the microscope slide surface. Capillaries for ablation tests were secured to the slide at multiple points so that multiple gaps could be cut on a single slide. After the epoxy cured, the microscope slide was placed on a translation stage (423 series; Newport; Irvine, CA) for laser ablation near the focal point of a fused-silica cylindrical lens (focal length, 10 mm; 01LQC407; Melles Griot, Carlsabad, CA) as illustrated in Figure 1.

The optimal distance between the capillary and cylindrical lens was determined by translating a test capillary along the axis of the laser beam from the Nd:YAG laser (ML-II; Continuum; Santa Clara, CA), cutting a series of gaps and locating the position that produced the smallest gap. A plano-convex lens (focal length, 100 mm; H45274; Edmund; Barrington, NJ) was used to focus the beam from a laser pointer ($\lambda$ = 650 nm; Quarton Inc.; His-Chih, Taipei Hsien, Taiwan) onto the capillary. The laser pointer was placed on a translation stage so that it could be moved in the same direction as the path of the Nd:YAG laser beam. The laser pointer was moved for each successive step during the location of the optimal distance between the capillary and the cylindrical lens. Once the optimal distance was located, a capillary could be reproducibly positioned at this point using the laser pointer as a reference. The second harmonic output from the Nd:YAG laser


(27) Emmer, A.; Roeraade, J. *Chromatographia* **1994**, *39*, 271−278.
(28) Amankwa, L. N.; Kuhr, W. G. *Anal. Chem.* **1993**, *65*, 2693−2697.
(29) Gallaher, D. L.; Johnson, M. E. *Appl. Spectrosc.* **1998**, *52*, 292−297.
(30) Chen, S.; Lillard, S. J. *Anal. Chem.* **2001**, *73*, 111−118.
(31) MacTaylor, C. E.; Ewing, A. G. *J. Microcolumn Sep.* **2000**, *12*, 279−284.
(32) Zhang, L.; Yeung, E. S. *J. Chromatogr., A* **1996**, *734*, 331−337.
(33) Gilman, S. D.; Pietron, J. J.; Ewing, A. G. *J. Microcolumn Sep.* **1994**, *6*, 373−384.
(34) Kelly, J. A.; Reddy, K. R.; Lee, C. S. *Anal. Chem.* **1997**, *69*, 5152−5158.
(35) Hardy, S.; Jones, P.; Riviello, J. M.; Avdalovic, N. *J. Chromatogr., A* **1999**, *834*, 309−320.
(36) Kostel, K. L.; Lunte, S. M. *J. Chromatogr., B* **1997**, *695*, 27−38.
(37) Zhu, R.; Kok, W. T. *J. Chromatogr., A* **1995**, *716*, 123−133.
(38) Wei, H.; Li, S. F. Y. *Anal. Chem.* **1998**, *70*, 5097−5102.
(39) Hornberger, H.; Weissmann, R.; Lutz, N. *Glastech. Ber. Glass Sci. Technol.* **1996**, *69*, 44−49.
(40) Ihlemann, J.; Wolff, B.; Simon, P. *Appl. Phys. A* **1992**, *54*, 363−368.
(41) Varel, H.; Ashkenasi, D.; Rosenfeld, A.; Wahmer, M.; Campbell, E. E. B. *Appl. Phys. A* **1997**, *65*, 367−373.
(42) Salleo, A.; Sands, T.; Genin, F. Y. *Appl. Phys. A* **2000**, *71*, 601−608.
(43) Roberts, M. A.; Rossier, J. S.; Bercier, P.; Girault, H. *Anal. Chem.* **1997**, *69*, 2035−2042.
(44) Rossier, J. S.; Schwarz, A.; Reymond, F.; Ferrigno, R.; Bianchi, F.; Girault, H. H. *Electrophoresis* **1999**, *20*, 727−731.
(45) Osbourn, D. M.; Lunte, C. E. *Anal. Chem.* **2001**, *73*, 5961−5964.

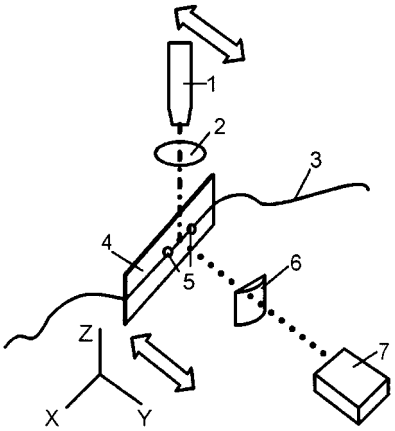


Figure 1. Schematic of the laser ablation system. Key: (1) laser pointer, (2) plano-convex lens, (3) capillary, (4) microscope slide, (5) epoxy, (6) cylindrical lens, and (7) Nd:YAG laser. Double arrows indicate the movement of the microscope slide and the laser pointer on separate translation stages for adjustment of the distance between the capillary and the cylindrical lens (diagram not to scale).

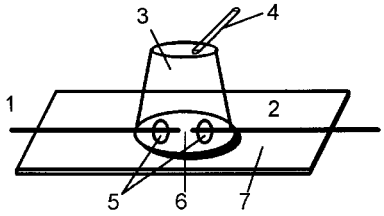


Figure 2. Schematic of a gap reactor. Key: (1) separation capillary, (2) reaction capillary, (3) gap reservoir, (4) Teflon tubing used for sample introduction, (5) epoxy, (6) capillary gap, and (7) microscope slide.

(532 nm) was used for laser ablation. A computer program written in LabView (National Instruments; Austin, TX) was used to control the frequency and number of pulses produced by the Nd:YAG laser. The pulses from the Nd:YAG laser were attenuated by a high-energy variable attenuator (935-3-OPT; Newport).

**Reactor Construction.** After construction of the gap, a reagent reservoir (~1.5 mL) was formed by sealing a polyethylene stopper from a 5-mL vial (03-339-27B; Fisher Scientific) with 5 Minute Epoxy.[33] A hole was drilled with a hot metal wire on the top of the polyethylene reservoir, and a 2-cm Teflon tube was fitted on the hole and attached with 5 Minute Epoxy as illustrated in Figure 2. Solutions were added to and removed from the reservoir by a syringe through the Teflon tubing.

**Gap Size Measurement.** Gaps created were examined using a video trinocular head zoom microscope (52353; Edmund), and an image was collected by a CCD camera (GP-KR222; Panasonic). The image was captured by VIDCAP 32 software (Microsoft) and saved as a single frame. The saved file was opened using Scion software (Scion Corp.; Frederick, MD), and the gap width was recorded in pixels using this software. The number of pixels was converted to micrometers by calibrating the software with a three-point calibration using a 0.01-mm standard micrometer (12-562-SM; Fisher Scientific).

**CE with LIF Detection.** Tests of gap performance were conducted by separating fluorescein and coumarin 334 and using LIF detection with a He−Cd laser (2056 MA03; Melles Griot; Santa Clara, CA) for excitation. The 325-nm line was removed by a 442 ± 10-nm band-pass filter (52620; Oriel, Stratford, CT), and the 442-nm beam was focused on the capillary by a fused-silica plano-convex lens (focal length, 12.7 mm; 4116; Oriel). Fluorescence was collected using a 20× microscopic objective (Edmund) and was filtered by a 465-nm long-pass filter (03FCG 465; Melles Griot). The fluorescence signal was spatially filtered by a 800-$\mu$m-diameter aperture (Oriel) and detected by a photomultiplier tube (PMT) (HC120; Hamatsu, Bridgewater, NJ). The PMT output was then filtered by a 50-Hz low-pass filter and sent to an analog-to-digital board (Lab-PC-1200; National Instruments). A computer program written in LabView was used for data acquisition. Data were acquired at 10 Hz. The acquired data were analyzed by Peak Fit (SPSS Inc., Chicago, IL). For postcolumn derivatization experiments, an Ar ion laser was used for excitation at 457.9 nm (1.5 mW; Lexel-3500; Lexel Laser, Inc., Fremont, CA), and two 495-nm long-pass filters (51292; Oriel) were used. The rest of the conditions were the same as for the He−Cd laser system above.

**Postcolumn Derivatization.** A gap reactor constructed from a single capillary (50-$\mu$m i.d./220-$\mu$m o.d.) was filled manually by injecting 50 mM borate buffer (pH 9.5) with a syringe. The capillary on each side of the gap was filled independently until buffer was observed to flow from the capillary into the gap. After the capillary was filled with borate buffer, the reservoir was filled with either the postcolumn derivatization solution or the running buffer. A positive high potential was applied at the injection reservoir, and the detection capillary was grounded. The gap reservoir was floated. The gap reservoir and the two ends of the capillary were set at the same height to minimize gravity flow. A 25-kV potential was applied for 20 min before the introduction of analyte. Electrokinetic injection was used for all experiments. A stock solution of naphathalene-2,3-dicarboxyaldehyde (NDA) (3.3 mM) was prepared in methanol and stored at 4 °C. The derivatization solution was prepared daily by diluting the stock solution to 1.0 mM NDA in 50 mM borate buffer (pH 9.5) and adding 4.5 mM 2-mercaptoethanol.[46] The final methanol concentration in the derivatization solution was 30%.

**Chemicals.** Fluorescein, α-lactalbumin, $\beta$-lactoglobulin A, $\beta$-lactoglobulin B, and transferrin were obtained from Sigma Chemical Co. (St. Louis, MO), and DL-aspartic acid and L-(+)-glutamic acid were obtained from Fisher Scientific. Boric acid was supplied by J. T. Baker Chemical (Phillipsburg, NJ). NDA was purchased from Fluka (Milwaukee, WI). 2-Mercaptoethanol, coumarin 334, and glycine were obtained from Acros (Pittsburgh, PA). All solutions and buffers were made in doubly distilled water.

**Safety Considerations.** The Nd:YAG laser used in this work can cause permanent and severe eye damage. Appropriate precautions should be taken when working with this laser, including the use of laser safety goggles and careful confinement of the beam. Caution should be used when working with high voltage for CE. Contact with the floated gap reactor should be avoided while the high voltage is turned on.

## RESULTS AND DISCUSSION

A simple system composed of a Nd:YAG laser, a cylindrical lens, and a capillary glued at two points to a microscope slide is used to cut small gaps (<20 $\mu$m) in a fused-silica capillary by laser ablation (Figure 1). The laser beam from the Nd:YAG laser is focused by the cylindrical lens to a line image on the capillary so

(46) Gilman, S. D.; Ewing, A. G. *Anal. Methods Instrum.* **1995**, *2*, 133−141.

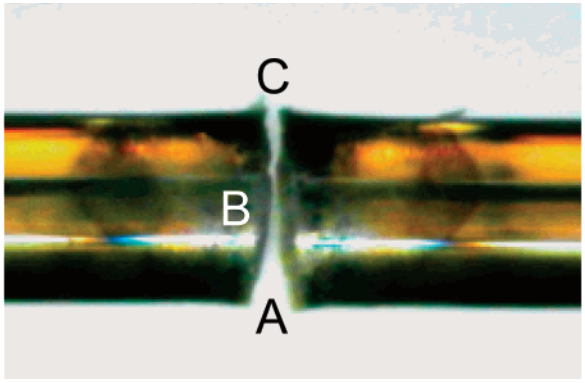


Figure 3. Photograph of a 10.9-$\mu$m gap (at B) in a 50-$\mu$m-i.d./220-$\mu$m-o.d. capillary created using 400 pulses at 15 Hz and 13.5 mJ/pulse. (A) Front, (B) center, and (C) rear of the capillary relative to the ablating beam.

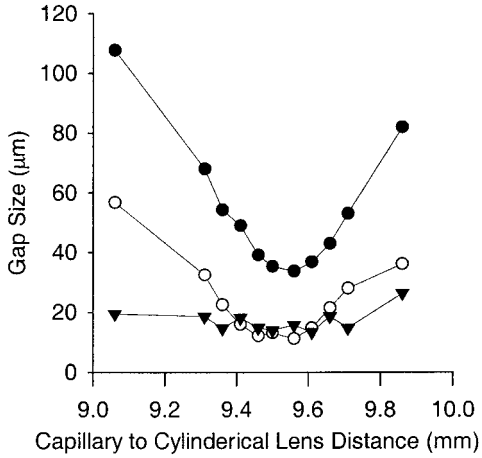


Figure 4. Effect of distance from the capillary to the cylindrical lens on gap size. (●) is the gap size at the front of the capillary nearest the cylindrical lens (A, Figure 3), (○) is the gap size at the capillary bore (B, Figure 3), and (▼) is the gap size at the rear of the capillary (C, Figure 3). Conditions: 50-$\mu$m-i.d./220-$\mu$m-o.d. capillary ablated by 400 pulses at 15 Hz and 13.5 mJ/pulse. Lines through the data were added as a visual aid.

that the laser light will ablate across the capillary bore along the *Z*-axis in Figure 1. Once the optimal capillary position for cutting is located near the focal point of the cylindrical lens, additional capillaries are placed at this same spot to reproducibly construct additional gaps. An optimized gap created using this method is shown in Figure 3.

Inconsistent results were obtained for initial attempts to cut gaps in capillaries using this approach despite the care taken to secure the capillaries with epoxy at a fixed distance from the surface of the microscope slide (~950 $\mu$m). It was determined that variability of the microscope slide thickness (±50 $\mu$m tolerance) resulted in inconsistent placement of the capillary relative to the optimal position with respect to the cylindrical lens. A laser pointer and a simple objective lens are used to overcome this problem. The beam from the laser pointer is initially focused to a small spot on the capillary with a plano-convex lens with the focal point at the height of the Nd:YAG beam used for capillary cutting. When the light from the laser pointer hits the surface of the capillary, light is scattered. The scattered light is imaged onto a screen placed behind the microscope slide relative to the Nd:YAG laser. Depending upon the position of the focused beam on the capillary (at the front, at the bore, or at the rear relative to the cylindrical lens) distinct images of the scattered light are observed on the screen. For consistency, the position at which light scattered from the rear side of the capillary was selected as a reference. Using this approach a capillary can be repositioned with an experimental uncertainty of ±2 $\mu$m.

Capillary ablation was carried out both with and without the polyimide coating on the capillary present at the point of ablation. The polyimide coating was removed by a gas flame for experiments with bare capillaries. Pulse energies of 8.0, 9.0, and 10.0 mJ/pulse were used for ablation using 400 pulses at 15 Hz with the polyimide removed. No cut was obtained using 8.0 mJ/pulse (three attempts), and only one completely cut gap was obtained using 9.0 mJ/pulse (seven attempts). A pulse energy of 10.0 mJ resulted in 87% complete cuts. However, the gaps obtained had large cracks and pieces missing, and the gap size and shape were not reproducible. Such laser-induced damage is expected using nanosecond pulses for ablation of fused silica.[39−42,47] No complete gaps were obtained (five attempts) using 400 pulses at 10.0 mJ/pulse and 15 Hz with the polyimide coating in place at the point of ablation. However, at a pulse energy of 13.5 mJ/pulse, gaps such as that shown in Figure 3 were reproducibly obtained. Although a higher pulse energy is required to cut gaps with the polyimide coating in place, the gaps produced contain fewer fractures and missing pieces. The structural support provided by the polyimide coating may reduce fracturing during ablation. All further gaps have been cut with the polyimide coating in place.

Determination of gap size and examination of gap shape were performed using a microscope, viewing the gap from the same relative position as that of the laser pointer, orthogonal to the Nd:YAG laser beam. An image of a typical, optimized gap is presented in Figure 3. Imaging from this direction provides the clearest indication of whether the gap has been completely cut, defined as cleavage from front to back without any polyimide coating or fused silica spanning the gap. This imaging approach enables the observation of three distinct sections of the gap. The part of the ablated gap nearest the cylindrical lens during ablation is labeled (A), the gap at the bore of the capillary is labeled (B), and the part of the gap farthest from the cylindrical lens is labeled (C). As shown in Figure 3, the gap is largest at (A) (34.9 $\mu$m) and smallest at bore of the capillary (10.9 $\mu$m). At (C), the gap is 11.9 $\mu$m. This shape resembles the shape of holes drilled in quartz plates by laser ablation in other studies.[40−42]

**Optimization of Gap Cutting.** The gap size at positions A, B, and C was studied as the distance between the cylindrical lens and the capillary was varied. The capillary was positioned from 9.06 to 9.94 mm from the front of the cylindrical lens. As seen in Figure 4, the gap size at the front (A) and at the bore (B) of the capillary decreases as the capillary approaches the focal point of the cylindrical lens. However, little change in gap size is observed at the rear of the capillary (C). The smallest gaps at the bore of the capillary (B) were obtained between 9.40 and 9.60 mm. A distance of 9.50 mm was selected for optimal ablation. This position was reproducibly relocated from experiment to experiment using the laser pointer reference.

(47) Stuart, B. C.; Feit, M. D.; Rubenchik, A. M.; Shore, B. W.; Perry, M. D. *Phys. Rev. Lett.* **1995**, *74*, 2248−2251.

The effects of varying laser pulse energy, pulse number, and pulse repetition rate were characterized to optimize the gap size and percentage of gaps successfully cut. The effect of varying the pulse energy between 12.0 and 14.0 mJ/pulse on the gap size has been studied at constant frequency (15 Hz) and number of pulses (400 pulses). Gap sizes (at the bore of the capillary) of 14.6 ± 1.9 ($n$ = 16), 13.9 ± 1.0 ($n$ = 17), and 14.6 ± 1.5 $\mu$m ($n$ = 16) were obtained for pulse energies of 14.0, 13.5, and 13.0 mJ/pulse, respectively. The percentages of completely cut capillaries obtained were 89% (16/18), 94% (17/18), and 89% (16/18) for pulse energies of 14.0, 13.5, and 13.0 mJ/pulse, respectively. The gap size and the number of completely cut capillaries showed no significant differences from 14.0 to 13.0 mJ/pulse. Below 13.0 mJ/pulse, the percentage of the completely cut capillaries dropped rapidly. No completely cut capillaries were obtained using a pulse energy of 12.0 mJ/pulse for three trials. Pulse energies above 14.0 mJ/pulse generated more damage (primarily cracks) in the capillary. A pulse energy of 13.5 mJ/pulse was selected for studying pulse number and repetition rate.

The effect of varying the pulse frequency on the gap size was studied. Pulse frequencies of 15, 7, and 1 Hz were used while constant pulse number (400 pulses) and pulse energy (13.5 mJ/pulse) were maintained. Gap sizes of 13.9 ± 1.0 ($n$ = 17), 13.5 ± 1.7 ($n$ = 14), and 15.6 ± 3.6 $\mu$m ($n$ = 12) were obtained for pulse frequencies of 15, 7, and 1 Hz, respectively. No significant difference in gap size was observed between cuts made at all three frequencies, but the percentage of completely cut capillaries dropped from 94% (17/18) to 78% (14/18) as the frequency was reduced from 15 to 7 Hz. The percentage cut dropped further to 71% (12/17) when the pulse frequency was reduced to 1 Hz. This may be a result of reduced heating at lower pulse rates.[48] Based on these data, a pulse frequency of 15 Hz (maximum for this laser) was used to study the number of pulses required for gap cutting. The total number of pulses was varied from 300 to 600 while the pulse energy (13.5 mJ/pulse) and pulse frequency (15 Hz) were kept constant. As the number of pulses increased from 300 to 600, the gap size increased from 11.8 ± 1.9 ($n$ = 11) to 14.6 ± 1.5 $\mu$m ($n$ = 18). The percentage of completely cut capillaries also increased from 61% (11/18) to 100% (18/18) as the pulse number was increased from 300 to 600. A pulse number of 400 was selected for further studies, as this value provided a high success rate (94%) and reasonably small gaps (13.9 ± 1.0 $\mu$m).

The reproducibility of the method was examined using the optimized cutting conditions (13.5 mJ, 400 pulses, and 15 Hz). A total of six different microscope slides each having six different cutting positions were used. An average gap size of 14.0 ± 2.2 $\mu$m ($n$ = 33) at the bore of the capillary (B) was obtained with 94% (33/35) of the capillaries being completely cut. No significant difference was observed between gaps cut on each slide. The average gap size obtained for the six positions on each slide ranged from 13.4 ± 2.1 ($n$ = 5) to 14.8 ± 4.6 $\mu$m ($n$ = 5).

**Gap Performance.** Separations of coumarin 334 and fluorescein were carried out in order to determine the efficiency of electrophoretic transport of analyte zones across the gap during an electrophoretic separation. Ten gaps were cut using the optimized conditions, and gap reactors were constructed as shown in Figure 2. Out of 10 gaps cut, 8 functioned properly and 1 was broken during construction. A 10 mM borate buffer (pH 9.6) was used in the gap reservoir and as a running buffer. Fluorescein (0.1 $\mu$M) and coumarin 334 (0.3 $\mu$M) were separated using this system with LIF detection.

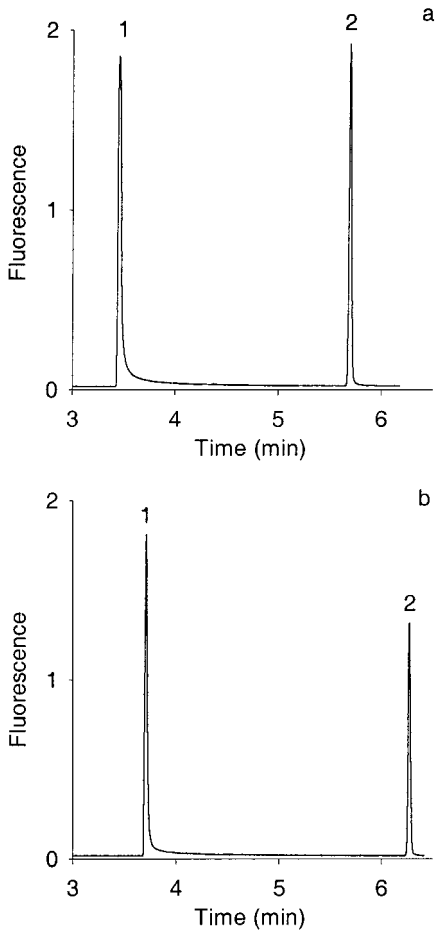


Figure 5. (a) Separation of 0.1 $\mu$M coumarin 334 (1) and 0.3 $\mu$M fluorescein (2) with a gap reactor (gap size at bore is 12.9 $\mu$m) and (b) the same separation without a gap reactor. Conditions: 79.0-cm total capillary length (a and b), 54.6 cm to detection window (a and b) and 53.2 cm to gap (a); 50-$\mu$m-i.d./220-$\mu$m-o.d. capillary; 3 s, 25-kV injection; 25-kV separation potential; 10 mM borate buffer at pH 9.6.

Figure 5 shows a separation of coumarin and fluorescein using a gap reactor (a) and a capillary without a gap (b). The gap reactor used here is reactor A in Table 1. The fluorescein peaks in (a) and (b) appear to be nearly identical in shape, but an increase in tailing and a decrease in peak height relative to the fluorescein peak are observed for coumarin 334 after traveling across the gap. This difference may be explained by the charge of fluorescein (−1) and coumarin 334 (0) and studies of electrophoretic transport across a capillary gap by Kuhr and co-workers.[26] This work suggests that charged species will be "focused" into the second capillary by the electric field across the gap. Coumarin 334 is uncharged and unaffected by the applied field; therefore, coumarin 334 will diffuse more readily out of the fluid stream between the two capillaries, resulting in more tailing of this peak compared to fluorescein. The separation efficiency was calculated for the coumarin 334 and fluorescein peaks and compared with a control using a capillary of the same length without a gap. The separation

(48) Bauerle, D. *Laser Processing and Chemistry*, 3rd ed.; Springer-Verlag: New York, 2000.

Table 1. Separation Efficiency for Gap Reactors[a]

| gap reactor | gap size (B) ($\mu$m) | theoretical plates $\times 10^{-3}$ | |
|---|---|---|---|
| | | fluorescein | coumarin 334 |
| A | 12.9 | 258 ± 15 | 26 ± 6 |
| B | 12.9 | 305 ± 39 | 61 ± 8 |
| C | 10.9 | 203 ± 36 | 21 ± 17 |
| D | 12.9 | 381 ± 43 | 46 ± 21 |
| E | 11.9 | 131 ± 5 | 26 ± 16 |
| F | 11.9 | 175 ± 24 | 71 ± 5 |
| G | 10.9 | 111 ± 7 | 16 ± 2 |
| H | 12.9 | 137 ± 11 | 33 ± 3 |
| average | 12.2 ± 0.9 | 213 ± 94 | 38 ± 20 |
| control (no gap) | | 308 ± 37 | 80 ± 11 |

[a] See Figure 5 for experimental conditions.

efficiency was calculated using the peak width at 10% peak height, the retention time, and the tailing factor.[49] The results for all eight gaps are summarized in Table 1. The number of theoretical plates for the gap reactors was reduced by 31% for fluorescein and by 52% for coumarin 334 in comparison with the control. A loss of 20% in theoretical plates was reported for 50 $\mu$M glycine labeled with *o*-phthalaldehyde for a single-capillary gap reactor with a gap size of 17 $\mu$m.[33] Improved separation efficiency (5% loss of efficiency, >400 000 theoretical plates) has been obtained with gap reactors by controlling the potential at the gap reservoir and applying a higher potential field in the reaction capillary.[8] However, we did not attempt to improve separation efficiency using this approach since our goal was to compare our gap reactors to results obtained with previous construction methods.

The electropherogram in Figure 6 shows the separation of a mixture of proteins and amino acids by CE with postcolumn derivatization using NDA and 2-mercaptoethanol as the post-column derivatization reagent.[46] The amino acids in this separation, glutamic acid (5) and aspartic acid (6), are ~100 times more concentrated than the proteins but give a similar fluorescence signal. This result is consistent with previous work using this reagent combination for postcolumn derivatization and likely results from a combination of several factors.[46] First, electrokinetic injection was used, so the two amino acid peaks will be relatively reduced due to injection bias. Second, the proteins may be labeled multiple times, resulting in a large signal relative to the amino acids. Finally, the relative reaction rates of the proteins and amino acids and the relative degradation rates of the fluorescent products may also contribute to the observed results. If the amino acids react more slowly than the proteins, or if their derivatives are less stable, this would contribute to the relatively small amino acid peaks. The NDA/mercaptoethanol derivatives are not suitable for precolumn labeling due to their instability.[36,46,50,51]

Glycine and transferrin were used to study the limits of detection for the method in order to allow a direct comparison

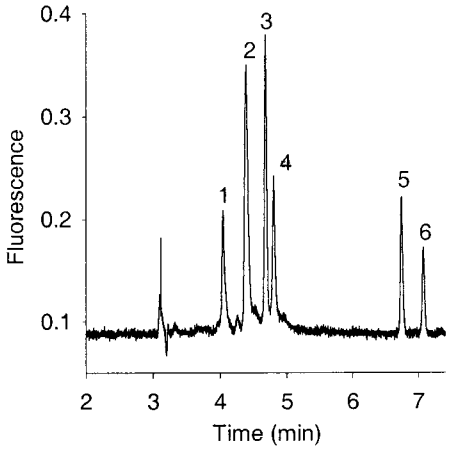


Figure 6. Separation of a protein and amino acid mixture using postcolumn derivatization with a gap reactor. Conditions: 70.0-cm total capillary length, 50.8 cm to detector and 49.4 cm to gap; 50-$\mu$m-i.d./220-$\mu$m-o.d. capillary; 10.9-$\mu$m gap size at bore; 3 s, 25-kV injection; 25-kV separation potential; derivatizing reagent, 1 mM NDA, 4.65 mM mercaptoethanol, 30% methanol in 50.0 mM borate buffer at 9.5 pH. Peaks: (1) 2.4 $\times$ $10^{-7}$ M transferrin, (2) 1.5 $\times$ $10^{-6}$ M $\alpha$-lactalbumin, (3) 8.5 $\times$ $10^{-7}$ M $\beta$-lactoglobulin B, (4) 1.6 $\times$ $10^{-6}$ M $\beta$-lactoglobulin A, (5) 2.0 $\times$ $10^{-4}$ M L-(+)- glutamic acid, and (6) 2.2 $\times$ $10^{-4}$ M DL-aspartic acid.

with previously reported results. The limits of detection for glycine and transferrin were determined to be 6 $\times$ $10^{-7}$ and 1 $\times$ $10^{-8}$ M, respectively, at 3 times the rms noise. Compared to the previously reported limits of detection, these values are approximately the same for glycine and a factor of 3 lower for transferrin using this reagent and a gap reactor.[46] The separation efficiencies for the peaks in Figure 6 ranged from 31 000 theoretical plates for $\alpha$-lactalbumin to 188 000 theoretical plates for aspartic acid.

## CONCLUSION

In this paper, we report a simple and rapid method for reproducible construction of a gap reactor for CE without micromanipulation under a microscope or chemical etching. In comparison to other methods of gap construction, this approach produces highly reproducible, perfectly aligned gaps. Comparable concentration limits of detection for glycine and transferrin were obtained in comparison to gaps constructed manually under a microscope. Further studies are underway to minimize the pulse energy and reduce the gap size and the damage to the capillary by using solvents as an aid for ablation.

## ACKNOWLEDGMENT

The authors thank Angela Whisnant, Debra Van Engelen, and Werner Kuhr for their helpful suggestions. This project was funded by The University of Tennessee and the National Science Foundation under Grant CHE-0094287.

Received for review November 16, 2001. Accepted January 23, 2002.

AC015693W

(49) Foley, J. P.; Dorsey, J. G. *Anal. Chem.* **1983**, *55*, 730−737.
(50) Montigny, P. D.; Stobaugh, J. F.; Givens, R. S.; Carlson, R. G.; Srinivasachar, K.; Sternson, L. A.; Higuchi, T. *Anal. Chem.* **1987**, *59*, 1096−1101.
(51) Dave, K. J.; Stobaugh, J. F.; Rossi, T. M.; Riley, C. M. *J. Pharm. Biomed. Anal.* **1992**, *10*, 965−977.